Dynamic properties of Lions' Gate suspension bridge

Rainer, J. H.; Van Selst, A.

Publisher's version / Version de l'éditeur:

Proceedings, ASCE/EMD Specialty Conference Dynamic Response of Structures: Instrumentation, Testing Methods and System Identification: 30 March 1976, Los Angeles, CA, USA, pp. 243-252, 1976

National Research Council Canada | Conseil national de recherches Canada

DYNAMIC PROPERTIES OF LIONS' GATE SUSPENSION BRIDGE

by J. H. Rainer and A. Van Selst

Reprinted, with permission, from
Proceedings, ASCE/EMD Specialty Conference
Dynamic Response of Structures: Instrumentation, Testing
Methods and System Identification
held at the University of California, Los Angeles
30 and 31 March 1976
p. 243 - 252

DBR Paper No. 700
Division of Building Research

Price 25 cents OTTAWA NRCC 15588

DYNAMIC PROPERTIES OF LIONS' GATE SUSPENSION BRIDGE

by

J.H. Rainer [I] and A. Van Selst [II]

INTRODUCTION

The Lions' Gate Suspension Bridge crosses the First Narrows of Burrard Inlet at Vancouver, British Columbia. The bridge, which opened in 1938, carries three lanes of vehicular traffic and two sidewalks. Because of the need for extensive repairs to the bridge deck and requirements for wider traffic lanes, a complete rebuilding of the deck structure is planned. This will result in the sidewalks being moved from inside the stiffening trusses to the outside. A new orthotropic road surface is to replace the present concrete and steel grid supported on steel beams and girders. Since changes in geometric and structural properties could influence the behavior of the modified bridge under wind loading, an aerodynamic investigation is being undertaken which includes wind tunnel section tests and a full aeroelastic model. To obtain some guidance in establishing the dynamic parameters for the model tests and the design calculations, measurements on the existing structure were carried out to determine its dynamic properties. This paper describes the measurement program and the results obtained, as well as comparisons between the observed values of natural frequencies and those from two different methods of calculation.

DESCRIPTION OF THE BRIDGE

The bridge consists of a main span of 1550 ft (473 m) and two side spans, each of 614 ft (187 m). The tower height is 361.5 ft (110 m) from top of concrete footing to the saddle points, with the road deck passing at mid-height. An elevation is presented in Fig. 1, and a typical cross-section with some structural properties in Fig. 2.

I Division of Building Research, National Research Council of Canada, Ottawa, Ontario, Canada.

II Buckland & Taylor Ltd., Consulting Engineers, Vancouver, British Columbia, Canada.

At the bridge center and at the north and south ends of the suspension bridge, traction rods connect the cable to the top chord of the stiffening truss. However, these traction rods were found to be somewhat loose. The two stiffening trusses are joined at the lower chords by floor beams that support the road deck, and by horizontal cross bracing that decreases in stiffness toward the center of the bridge. The trusses, together with the cross bracings and the decking, thus effectively form an open channel section. The trusses rest on fixed bearings at the N and S supports of the bridge and have sliding bearings at the towers. The girder has a vertical curve with rise of 22.3 ft (6.8 m) from the tower to the bridge center line.

MEASUREMENT PROGRAM

The measurements were performed in two main stages: Phase I was carried out during the winter of 1974-75, and Phase II, in September 1975. The subsequent description and results obtained refer to Phase II, except where otherwise noted.

Instrumentation

The motions of the bridge were monitored with battery-powered servo-drive accelerometers of 5 V/g sensitivity. These were mounted on brass bases and placed on the top flange of the cross beam close to the inside of the stiffening truss at the numbered locations shown in Fig. 1. Cables carried the signals to the recording station in the observation cabin at the bridge center. D-C compensation was applied, the signals passed through 1 Hz low pass filters and 20 dB amplifiers and were recorded on a 7-channel FM tape recorder. The transducers, signal conditioning and recording channels were calibrated in the laboratory and a static inversion check of the transducers was performed at the recording site.

Station 1N was used as a reference; the remaining stations were covered by successively moving the transducers to those stations. A special run was made with transducers placed at Stations 2N and 2S.

Ambient Vibrations. - Ambient vibrations during Phase II consisted of vehicular traffic only, mainly passenger cars and transit buses. Wind speeds ranged from zero to about 5 mph (8 km/h). During Phase I, measurements were also made under various wind conditions during early morning hours when traffic was minimal or absent. One limited set of measurements was obtained at winds gusting to 50 mph (80 km/h). For each setup the motions were monitored for approximately 45 min.

Vehicle Impacts. - A series of simulated impacts were applied to the bridge from a single rear axle sand truck and a small passenger car. The truck was driven in the outside lane at about 10 mph, swerved normal to the bridge and brought to a sudden braking stop. This produced torsional and lateral responses of the bridge. Another simulated impact test for torsional and lateral vibrations consisted of a small car driven normal to the roadway and brought to a sudden braking stop. Vertical impact responses were induced by slowly driving the rear wheels of the truck off a 6-in. (15-cm) ramp. However, this proved to be successful in only one of three attempts. Driving the truck from the main span onto the side span at approximately 40 mph (64 km/h) produced some satisfactory vertical motions.

Analysis of Data

Ambient Vibrations. - The ambient vibration data were analyzed on a 500-line real-time spectrum analyzer using tape speeds of 8, 10, and 16 times the recording speed and with 2 and 4 spectrum averages. Phase relationships between two stations were obtained by addition and subtraction of the respective signals. The amplitude and phase relationships were also confirmed by cross-spectral density calculations using 512 points and four spectrum averages.

Impact Response. - The impact response signals were digitized and analyzed on a digital computer using FFT routines. The time decay curve for various modes of vibration was obtained by inverting into the time domain the filtered spectrum for a particular modal frequency band. From this decay, modal damping was computed using the log decrement relationship.

CALCULATIONS OF MODAL PROPERTIES

Two methods were used to calculate the modal properties of the bridge: a continuum model, where the solutions to the differential equations describing the vibration problem are evaluated, and a lumped mass, linear stiffness model, for which eigenmodes were found.

Continuum model. - The theory for vibration of suspension bridges as presented by Selberg (3) was utilized in calculating the mode shapes and frequencies for the existing bridge. The following assumptions are made to simplify the treatment of the mathematical theory: a) axial deformations of towers and girder are neglected; b) the individual hangers are replaced by an equivalent membrane having no shear resistance; c) dead load is uniformly distributed along the span, implying a parabolic cable profile; d) girder has constant stiffness within each span; e) curvature of girder is negligible compared to cable sag; f) shear deformation in girder is negligible; g) deflections are small, i.e., linear displacement theory is used. The solution of the differential equations is a rapidly converging infinite series. A general computer program was written to solve the series by a trial and error method utilizing the first 5 terms for the side spans and 7 terms for the main span. The torsional modal properties were obtained analogously to the vertical ones by replacing the vertical stiffness and mass with the torsional stiffness and mass moment of inertia of the girder. The full torsional stiffness of the roadway is assumed to be activated and the traction rods are assumed to be unstressed.

The above method is similar to the theory presented earlier by Bleich et al. (1) but is more refined.

Lumped mass, linear stiffness model. - The stiffness matrix for the discrete model of some 750 members and 400 joints having over 1,000 degrees of freedom was assembled with a space-frame analysis program. Symmetry properties along the length and the width of the bridge were utilized so that only one quarter of the structure needed to be encompassed. The eigenvalue problem with the diagonal mass matrix was solved by a sweeping technique.

The method of analysis of the problem implies linear displacement theory. The torsional rigidity used for the bridge girder includes full participation of the roadway and stringers and the assumption that the expansion joints have seized.

Girder bearings at the towers are taken as fixed and the traction rods are assumed to be ineffective. These assumptions were found to best fit the experimental data.

RESULTS

The results of the measurements and calculations are presented in Tables 1, 2 and 3 for each identified mode. The measuring points on the interpolated modes shapes are shown by circles for the vertical and torsional displacements, and triangles for horizontal girder displacement. Damping values are given where possible, as well as the computed frequencies from the two mathematical models already described. The damping values from ambient vibrations were calculated using the method of half-power band width. Damping values calculated from the filtered decay curves vary slightly over the length of the decaying vibration record and consequently the values near the beginning of the impact and those after about 15 cycles are given. A correction was applied to the amplitudes of the decaying signal of the Phase I measurements by subtracting the amplitudes of the ambient signal due to wind excitation.

Categorization of Modes

The normal modes identified in the measurement program have been categorized into vertical, horizontal and torsional modes. However, the usual clear distinction between horizontal and torsional modes becomes obscured because both torsion and horizontal motion is present in most of these modes. Consequently, only the lowest mode, which is clearly identifiable as a horizontal mode, was designated as a horizontal mode, and all other modes with torsional components were designated as torsional modes.

Vertical Modes. - A sample set of Fourier spectra of vertical signals monitored at Station 1N are shown in Fig. 3. The modes associated with the various spectrum peaks are indicated near the top of the figure.

The vertical mode shapes, together with relevant damping values and the calculated frequencies, are presented in Table 1. The modes are presented sequentially according to increasing frequency. It is believed that in the vertical direction the modes identified represent a complete set of the major natural modes of vibration for the suspension bridge.

Horizontal Modes. - Because the horizontal motions are coupled with the torsion of the deck and towers and vice versa, a pure horizontal mode is unlikely to occur. In fact, only the lowest horizontal mode at 0.12 Hz presented in Table 3 was without measurable rotations under ambient vibrations. Only during the severest impact tests could rotational components be detected for this mode.

Torsional Modes. - The horizontal components of the modes shown by dash-dotted lines in Tables 2 and 3 give the modal amplitude on the top flange of the floor beam, i.e., just below the roadway level. The plotted torsional component shown by solid lines represents the sum of the vertical motions at the inside of the stiffening truss.

Since the accelerometers in the horizontal direction are sensitive to angular movements, a correction has to be applied to the measured horizontal component of

Table I: Dynamic Properties of Vertical Modes

Item No.		1	2	3	4	5	6	7	8
Measured Mode Shape		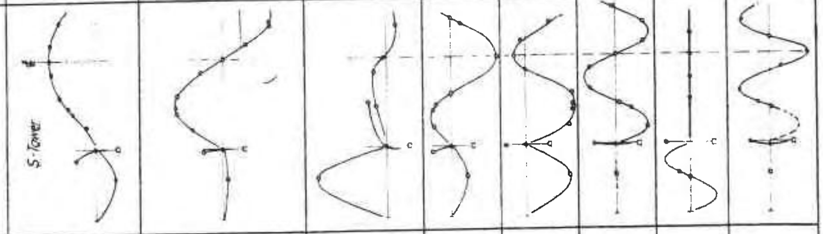							
Measured Frequency, Hz		0.200	0.225	0.30	0.358	0.420	0.590	0.760	0.845
Calculated Frequency Hz	Lumped Parameter	0.199	0.214	0.298	0.343	0.422			
	Continuum Model	0.185	0.214	0.273	0.345	0.408			
Damping Ratio, % critical, from	Fourier Spectra	1.7	1.6	1.7	1.0	0.7	0.6		0.6
	Impulse Decay	0.9*, 0.6* 1.1**, 0.9**	0.9*, 0.8* 1.05**, 0.95**						

* Uncorrected ** Corrected for ambient vibrations

Table 2: Dynamic Properties of anti-symmetric Torsional Modes

Item No.		1	2	3	4	5	6
Measured Mode Shape —•— Difference of Vertical Motion (East + up) –▲– Horizontal (+ to West)		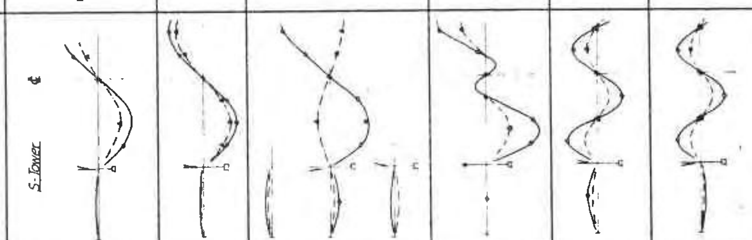					
Measured Frequency, Hz		0.310	0.32 (0.33)	0.495 0.515 0.507	0.600	0.745	0.765
Calculated Frequency, Hz	Lumped Parameter		0.317	0.463	0.568		
	Continuum Model		0.32 H* 0.411				
Damping Ratio from Fourier Spectra % critical			1.25	0.79			

* Calculated horizontal mode

the mode shape. This correction depends on the modal frequency and the amplitude of the angular motion at the measuring point. No correction could be applied to the modal amplitudes at the tower tops for the vertical and the torsional modes. Consequently, the plotted tower amplitudes are too large.

A sample spectrum of the rotational component for Station 1N is shown in Fig. 4. The anti-symmetric and symmetric torsional modes that could be identified are presented in Tables 2 and 3, respectively, together with damping values and theoretical frequencies where available. As can be seen, every torsional mode

Table 3: Dynamic Properties of Symmetric Torsional and Horizontal Modes

Item No.		1	2	3	4	5	6	7	8
Measured Mode Shape —o— Difference of Vertical Motion (East + up) —·▲— Horizontal (+ to West)		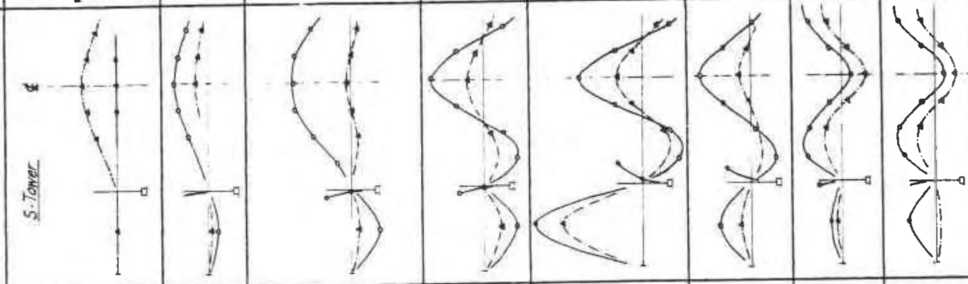							
Measured Frequency, Hz		0.12	0.36	0.38 (0.37, 0.39)	0.44	0.465	0.475	0.525	0.535
Calculated Frequency, Hz	Lumped Parameter	0.125		0.364		0.441*	0.477	0.533	
	Continuum Model	0.12 H**		0.347			0.593	0.646	
Damping Ratio, % critical from	Fourier Spectra	3.3	1.7	0.9	0.34		0.63	0.57	
	Impulse Decay	3.0 3.9		1.3, 1.6					

Item No.	9	10	11	12	13	14	15
Measured Mode Shape	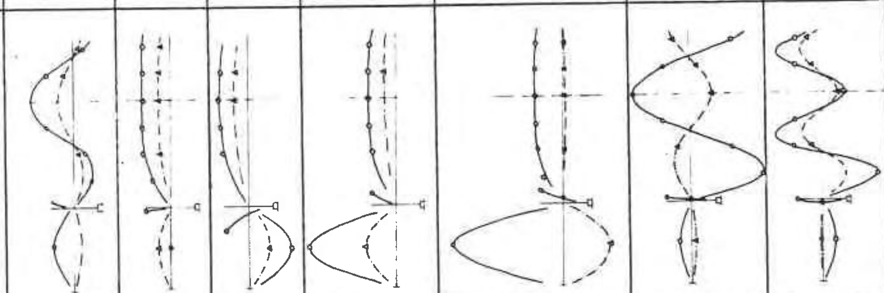						
Measured Frequency, Hz	0.555	0.615	0.635	0.65	0.715	0.94	1.00
Calculated Frequency, lumped Parameter Model, Hz		0.575		0.618	0.654		

* Mainly side span motion ** Computed horizontal mode

is also accompanied by a horizontal component.

DISCUSSION

Identification of Modes

Although the identification of the vertical mode shapes was fairly straightforward, the identification of the torsional modes proved to be a difficult task. Some of the reasons are: first, the coupling of torsion and horizontal motion obscured the usual clear distinction between horizontal and torsional modes; secondly, a large number of closely spaced modes appeared in the spectra, which to some extent influenced each other's spectral amplitudes; and thirdly, some of the modes had such small amplitudes that the limits of resolution of measurement and analysis equipment were approached.

The large number of torsional modes can be traced to the asymmetric stiffness properties of the U-section formed by the stiffening trusses and the road deck with horizontal crossbracing. Since, conceptually at least, various combinations of independent rotational and horizontal motions of side spans and main span are possible, the appearance of a large number of independent modes is perhaps not surprising. The close spacing of the modes requires high resolution spectrum analysis and consequently long recording sessions. No noticeable differences were found in the spectra of the signals recorded under traffic excitation or predominant low speed wind excitations or the strong wind excitation, although a more detailed examination of the latter has yet to be undertaken.

Some of the unresolved aspects on the identification of torsional modes are the following.

1. Multiple frequencies with substantially the same mode shapes were found near 0.32, 0.38, 0.51 and 0.94 Hz. Whereas some of these modes had different phases of sidespan and tower motions, others exhibited no noticeable differences.

2. From an examination of various Fourier and cross-spectral calculations, it is suspected that another symmetrical torsional mode exists very close to the symmetric mode at 0.465 Hz and another one near the asymmetric mode at 0.507 Hz. However, they could not be identified. It is thought that the plotted mode at 0.465 Hz is actually a composite of two modes, one a dominant side span mode, and the other a dominant main span mode.

A possible reason for the presence of multiple frequencies near 0.32, 0.38, 0.51 and 0.94 Hz might be the changing restraints as the tie rods begin to tighten and the bearings slip owing to changing loading conditions on the bridge.

Comparison of Measured and Calculated Frequencies

As the results in Table 1 indicate, there is generally excellent agreement between the measured and calculated frequencies for the vertical modes for both the continuum model and the lumped parameter model. The slightly lower calculated frequencies for the continuum model may in part be due to the necessary simplifications in the theory, such as constant mass and stiffness properties of the girder and neglecting the camber.

The frequency for the lowest horizontal mode, Item I in Table 3, also shows good agreement between calculations and measurements. As the continuum theory for the horizontal modes does not take account of coupled horizontal-torsional motion, the agreement for the higher modes can be expected to become less satisfactory.

For the frequencies of the torsional modes presented in Tables 2 and 3, the calculated values for the continuum model show substantial differences from measured ones. Reasons for this may be the difficulty in achieving realistic estimates for torsional stiffness of the girder and the assumptions of constant properties in each span. Furthermore, as mentioned previously, since the continuum theory does not account fully for coupled torsional-horizontal motion, a consistent agreement between measurements and calculations cannot be expected.

Damping

The simplest method of obtaining modal damping values is to calculate them from the half-power bandwidth of power (or Fourier) spectrum peaks. Unfortunately this method has some potential shortcomings when applied to the structure under consideration. First, changing loading conditions on the bridge cause small variations in the frequencies. These result in a widening of the resonance peak and thus yield damping values that may be too high. Averaging a number of sequential spectra is highly desirable for a proper definition of the spectrum peaks, but this accentuates the potential problem of getting wider peaks due to slight frequency shifts. Secondly, for some of the modes it is difficult or impossible to find a spectrum peak whose width can be properly measured. Where two modes nearly coincide an entirely erroneous picture may emerge if this is not recognized. Finally, amplitude dependence of damping cannot be delineated from the half-power bandwidth.

Although a forced resonance test would possibly yield the most reliable values of damping, it is impractical for this type of structure. However, the vibration decay from a simulated impulse can be used to obtain damping values. Attention should be paid to the following aspects: a) the presence of ambient vibrations should be recognized and possible corrections made; b) amplitude dependence of damping can be taken into account by calculating damping values at various points along the decay curve; and c) when two or more modes fall very close to each other, the vibration decay curve may be affected by modal interference and therefore the damping values obtained have to be interpreted with caution. This applies to the torsional mode at 0.38 Hz, where the damping values derived from the impulse curve are thought to be somewhat higher than if the individual frequency components could have been separated.

The damping values determined for this bridge are generally lower than those reported for two other suspension bridges (2).

CONCLUSIONS

Both the ambient vibration survey and the impact tests proved useful and complementary in obtaining dynamic properties of the bridge. For this particular structure, however, neither method by itself appears to be able to provide entirely consistent values of damping. Further efforts toward obtaining better damping values for suspension bridges are indicated.

The modal frequencies and mode shapes computed from the continuum model and the lumped parameter model showed excellent agreement with the measured values for the vertical and the lowest horizontal modes. Larger differences were encountered for the torsional modes, particularly for the continuum model. This is ascribed in part of the uncertain constraints that exist in the structure. The assumptions inherent in the continuum model do not appear to represent adequately the torsional behavior of this particular suspension bridge.

Acknowledgement

The Lions' Gate Bridge is owned by the Department of Highways of British Columbia. The cooperation of the Department in the measurement program is gratefully acknowledged, as is their permission to publish the paper. Structural consultants for the bridge modifications are Buckland and Taylor Ltd. of Vancouver, B.C. The assistance of their staff and of R.G. Diment, M. Jacob and E.C. Luctkar of the Division of Building Research of the National Research Council of Canada is also gratefully acknowledged. The results using the lumped mass, linear stiffness model were obtained by Hooley Engineering, Vancouver, B.C.

Portions of the measurements were taken while the first author (HJR) was on staff posting at the Faculty of Applied Science of the University of British Columbia, Vancouver, B.C.

References:

1. Bleich, F., et al, "The Mathematical Theory of Vibration of Suspension Bridges", Bureau of Public Roads, Department of Commerce, Washington D.C., 1950.

2. McLamore, V.R., Hart, G.C., and Stubbs, I.R., "Ambient Vibration of Two Suspension Bridges", Journal of the Structural Division, ASCE, Vol. 97, No. ST 10, Proc. Paper 8454, Oct. 1971, pp. 2567-2582.

3. Selberg, A., "Oscillation and Aerodynamic Stability of Suspension Bridges", Acta Polytechnica Scandinavica, Civil Engineering and Building Construction Series No. 13, Trondheim, Norway, 1961.

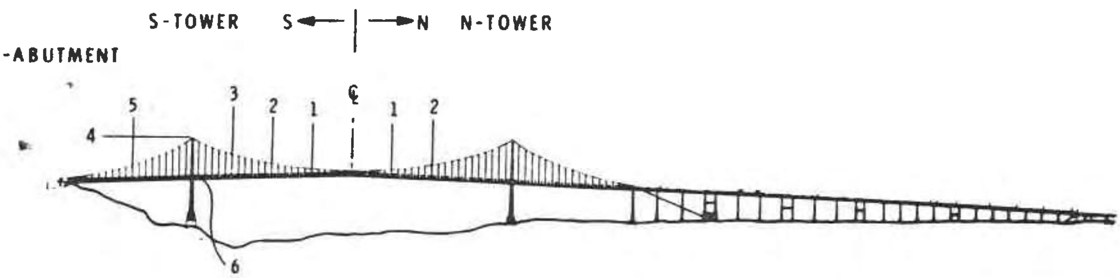

FIGURE 1

ELEVATION OF BRIDGE SHOWING MEASUREMENT STATIONS

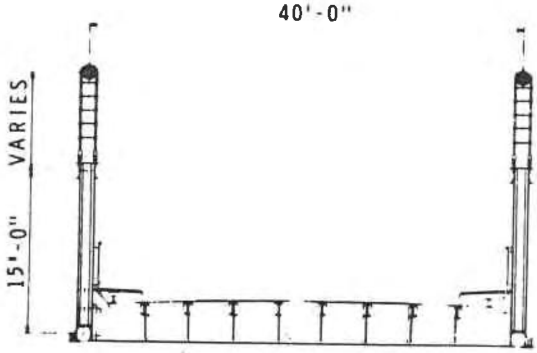

Data for Bridge:

Total Cable area = 144.9 in^2

Average:
- Bridge weight = 4.336 kip/ft for side span
  = 4.732 kip/ft for main span
- Mass Moment of Inertia about Center of Gravity = 31.0 kip sec^2 for side span
  = 37.0 kip sec^2 for main span

FIGURE 2

CROSS SECTION AND STRUCTURAL CONSTANTS

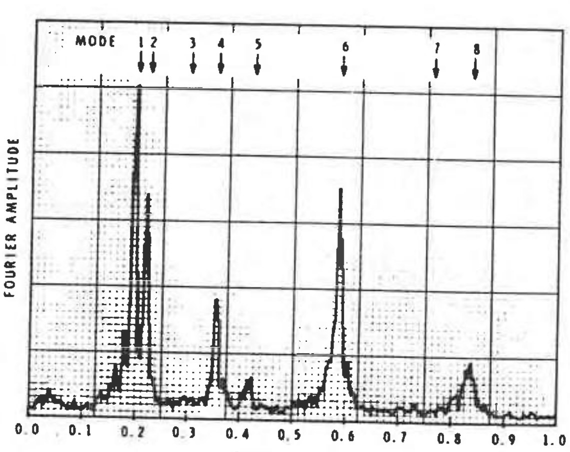

FIGURE 3

FOURIER AMPLITUDE SPECTRUM FOR VERTICAL MOTION AT STATION 1N

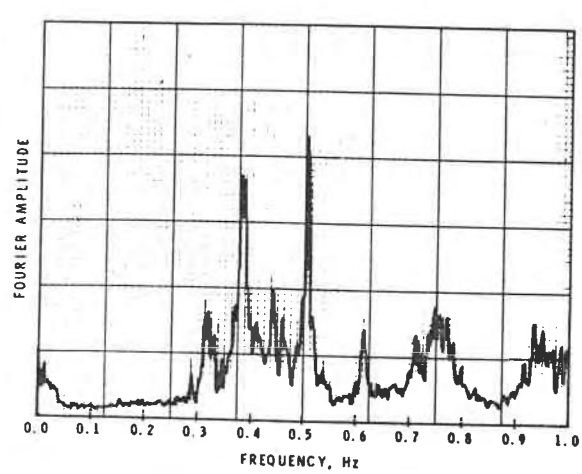

FIGURE 4

FOURIER AMPLITUDE SPECTRUM FOR TORSION AT STATION 1N